

16th Australasian Fluid Mechanics Conference
Crown Plaza, Gold Coast, Australia
2-7 December 2007

Enabling Micro Synthetic Jet Actuators in Boundary Layer Separation Control Using Flow Instability

Guang HONG

Mechatronic and Intelligent System Group, Faculty of engineering
University of Technology Sydney (UTS), NSW 2007, AUSTRALIA

Abstract

Research on synthetic jet actuators (SJAs) has shown great potential of using SJAs in control of boundary layer flow separation to reduce the drag and increase the efficiency of aerodynamic devices. The challenge lies in developing an actuator not only small, light, robust and economic, but also capable of reaching the control objectives. This paper presents an idea of using the flow instability to enhance the actuation of a SJA. In the case of controlling laminar separation, the SJA is used to trigger frictional Tollmien-Schlichting (T-S) instability. At a forcing frequency strategically determined, the triggered T-S instability which is originally weak can be enhanced by the frictionless Kelvin-Helmholtz (K-H) instability of the baseline flow, until the T-S instability becomes substantially strong to resist the separation. The effective actuation of a SJA in resisting laminar separation caused by adverse pressure gradient in a boundary layer is demonstrated by experimental results of profiles of mean and fluctuating velocities. The orifice diameter, which is the characteristic dimension, of the SJA is 500 μm . The forcing voltage is only $\pm 7.5\text{V}$., and the forcing frequency is 100 Hz. The Reynolds number is in a range of $1.78 \times 10^5 \sim 2.24 \times 10^5$. Boundary layer properties are used to understand the associated physics, and disturbance intensity is first time used to evaluate the effectiveness of the SJA. Analysis of the experimental results led to the conclusion that flow instability plays a critical role in enabling a micro SJA and also in making the control effectiveness less dependent or independent of the detailed structure and size of the actuator.

Introduction

MEMS-based boundary layer flow control has been led by Ho and Tai [7]. The 'flexible skin' developed by Huang et al. [11] has represented one of the most significant results in MEMS for flow control. Synthetic jet actuators (SJAs) have emerged as a micro-electro-mechanical system with potential applications ranging from separation and turbulence control to thrust vectoring, and augmentation of heat transfer and mixing. A synthetic jet has been known as a zero-net-mass but non-zero momentum fluid flux generated by a device such as a piezo-oscillator. Research work on SJAs has shown great potential of using SJA in active control of boundary layer separation in order to reduce the drag and increase the efficiency of aerodynamic devices [1,5]. Using SJAs to control flow separation was considered as the enabling means for the next-generation of UAVs and advance air mobility systems [12].

The use of synthetic jets to control flow separation in a boundary layer is based on the idea of accelerating the transition from laminar to turbulence which is more capable of resisting laminar separation. In the most recent publication, Gilarranz et al reported their work on developing a high-power synthetic jet actuator which acted as a reciprocating air compressor with a crank system and six pistons [3]. The maximum power consumption of this synthetic jet actuator was 1200W and the peak jet velocity was 124 m/s. They also reported the application of this newly

developed synthetic jet actuator to flow separation control over a NACA 0015 wing in conditions with a freestream velocity of 35 m/s and a Reynolds number of 8.96×10^5 . Their results showed that the synthetic jet actuation successfully decreased the drag and increased the maximum lift coefficient by 80% when the angle of attack was varied from 12 to 18 degree [4].

To develop an effective and efficient synthetic jet actuator, issues such as compactness, weight and power density need to be addressed. Addressing these issues requires the understanding of the physics in the synthetic jets' actuating process. This understanding will also be needed for developing the control strategies. As indicated in [3], in most laboratory demonstrations, the SJAs are either too big or too weak. Therefore, the challenge is to develop an actuator that is not only small, light, robust and economic, but also capable to reach the control objectives. One way to do this is to use the instability of the base flow to enhance the actuation which is decided by the controller [8,9,15]. In the case of controlling laminar separation using SJAs, the actuation is to use the synthetic jet to trigger T-S instability. This triggered flow instability may be originally weak but can be enhanced by the K-H instability of the base flow when the forcing frequency of the SJA is 'right', until the triggered instability becomes substantially strong and effective to meet the control purpose. Based on a numerical investigation, it was claimed that a new instability mechanism was identified which amplified small-amplitude 3-D disturbances in the reattachment zone when the separation bubble was large enough [13]. The present paper aims to disseminate an idea of using flow instability to make the SJA effective, which is essential for developing micro SJAs.

Low Power Synthetic Jet Actuator

The SJA used in the present study is schematically described in Figure 1. It consists of a membrane located at the bottom of a small cavity which has an orifice in the face opposite the membrane. The actuator membrane is a thin circular brass disc, 250 μm in thickness, held firmly at its perimeter. A piezoceramic disc is bonded to the outside face of the membrane. The lowest resonant frequency of the membrane is 900 Hz and its lump sum capacitance is approximately 140 nF. The SJA was installed underneath the wall surface over which the boundary layer flow is controlled. Its orifice open to the boundary layer flow has a diameter of 500 μm . More details of the SJA are given in [8].

The experiments were performed in the low speed wind tunnel in the Aerodynamics Laboratory at the University of Technology, Sydney. As shown in Figure 2, in the working section, a fairing was set above a flat aluminium plate with its angle adjustable for establishing the desired pressure gradient, similar to that of a diffusion compressor blade. The flat plate, located 1200 mm from the working section entrance, has a high quality surface finish. The leading edge of the upper surface is of slender elliptical form and the plate has a 0.250 negative incidence to avoid leading edge separation. In operation, as shown in Figure 2, the SJA was driven by a sine wave signal generated by a standard electrical

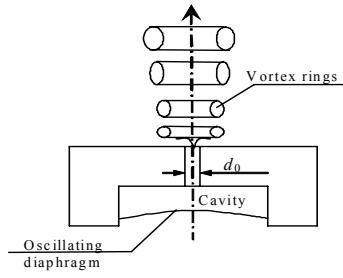


Figure 1. Schematic diagram of a synthetic jet actuator operating in a quiescent condition

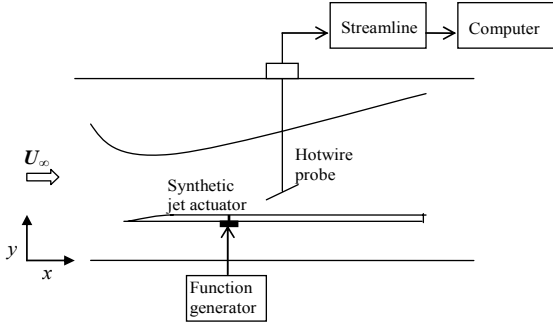


Figure 2. Side view of the experimental setting in the working section

function generator. As reviewed above, a micro actuator needs to be not only effective but also efficient. To be efficient, a SJA needs to be driven at the lowest forcing power. In the experiments, the peak-to-peak amplitude of the sine wave signal driving the SJA, called forcing amplitude, was only ± 7.5 V., and the frequency of the sine wave signal, called forcing frequency, was 100 Hz. This forcing frequency was chosen as one in the lower range of the T-S instability. When the SJA is in operation, an air jet is synthesized by oscillatory flow in and out of the cavity through the small orifice open to the boundary layer.

Demonstration of Separation Control

Sample experimental results will show the effective elimination of a laminar separation bubble by a SJA. The streamwise velocity was measured, using a Dantec hot wire anemometry, in the boundary layer over the upper surface of the flat plate. The ‘Streamline’ shown in Figure 2 was a package of software and hardware for interfacing between the computer and the hotwire probe and for data acquisition. The probe was traversed in streamwise (x) and normal (y) directions. A dial gage with a least count of 0.01 mm was used to adjust the probe’s position in y direction. The reflection of the probe tip, under a concentrated light source, was used for accurate probe positioning. The sample rate was 6 kHz, and the sample size of each realization was 4096. The axial center of the orifice of the SJA was defined as $x = 0$ mm. Measurements were made at $x = 40 - 160$ mm downstream of the SJA ($X_0 = 0.345 - 0.465$ m in Figure 3) at 20mm intervals.

Static taps were located every 25 mm along the streamwise centerline of the flat plate for pressure measurement using a multi-tube manometer. Figure 3 shows the pressure coefficient, c_p , calculated from the measured static pressure along the streamwise centerline at a free stream velocity of 8.0 m/s measured at the position with minimum pressure. X_0 is the distance from the leading edge of the flat plate. The minimum pressure is at the position $X_0 = 0.285$ m, and the centerline of the orifice of the SJA is at $X_0 = 0.305$ m. Hatman and Wang developed a prediction model for distinguishing three separated-flow transition modes, transitional separation, laminar separation-short bubble and laminar separation-long bubble [6]. The first mode involves transition starting upstream of the separation point, and the latter two have the onset of the transition

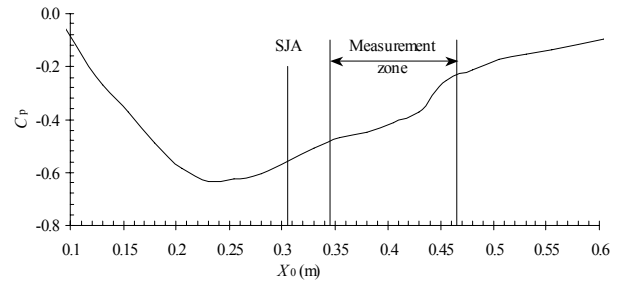


Figure 3. Streamwise pressure distribution

downstream of the separation point by inflexional instability. The separated flow transition in the current study belongs to the second mode, laminar separation-short bubble, as identified later with results in Figures 4 and 5.

Figure 4 demonstrates that the SJA successfully resists the laminar separation in a boundary layer with an adverse pressure gradient, by comparing the mean and fluctuating velocity profiles when the SJA is switched on and off. The Reynolds number, based on the local external velocity and distance to the leading edge of the flat plate, in the measurement zone is $1.78 \times 10^5 \sim 2.24 \times 10^5$. The mean velocity, \bar{u} , is normalized by the local external velocity, U , and the normalized mean velocity is denoted by \bar{u}/U . The fluctuating velocity, u' , is calculated as

$$u' = \sqrt{\frac{\sum_{i=1}^N (u_i - \bar{u})^2}{N}} \quad (1)$$

Where u_i is the i th sample data of the instantaneous streamwise velocity, \bar{u} is the sample mean of the streamwise velocity, and N is the sample size of one realization. Table 1 provides the distance from the axial center of the orifice of the SJA to the measurement station as numbered in Figure 4.

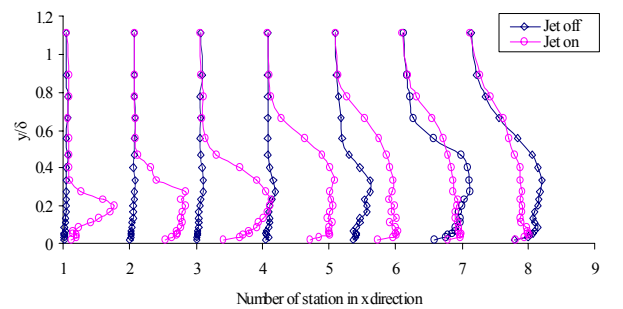
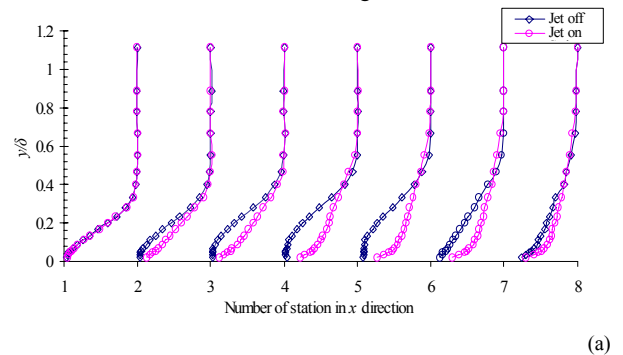


Figure 4 Comparison of experimental results when SJA is switched on and off. Forcing amplitude = ± 7.5 V., Forcing frequency = 100 Hz. See Table 1 for measurement positions in x direction. (a) Normalized mean velocity profiles, (b) Normalized fluctuating velocity profiles.

Table 1 Distance between the jet and the measurement station

No. of measurement station in x direction	1	2	3	4	5	6	7
Distance to the SJA (mm)	40	60	80	100	120	140	160

The mean velocity profiles in Figure 4(a) show how the SJA works to resist the flow separation, while the fluctuating velocity profiles in Figure 4(b) show why. In the condition with the jet off, at the x positions from 60 mm to 120mm, the mean velocity profile at small y/δ positions is quite ‘normal’ to the wall, and the velocity profile has an inflection point. The separation point is located between $x = 40$ mm and $x = 60$ mm, and this separation continues to a position between $x = 120$ mm and $x = 140$ mm. The fluctuating velocity profiles with jet off show that the separation is laminar and the transition occurs at about the center point of the separation bubble, between $x = 100$ mm and $x = 120$ mm. Following a short transition, reattachment of the separation bubble occurs at a position between $x = 120$ mm and $x = 140$ mm.

In the conditions with the synthetic jet on, the inflexion points on the mean velocity profiles disappeared. This is due to that the transition occurs at a position upstream of the natural separation point in the base flow, as shown in Figure 4(b). At $x = 40$ mm, although the mean velocity profile is not significantly modified yet, the fluctuating velocity has been generated by the synthetic jet actuation at $y/\delta = 0.07 \sim 3.4$. The fluctuating velocity increases in both streamwise (x) and normal (y) directions until it reaches the position of $x = 100$ mm which is close to the natural transition point of the base flow, as identified later with Figure 5. Following that, the fluctuating velocity decreases downstream. It is worth to note that at $x = 160$ mm, the mean velocity profile with the jet on is ‘fuller’ than that with the jet off, but the corresponding fluctuating velocity with the jet on is less than that with the jet off.

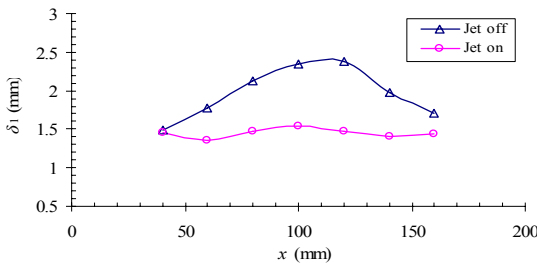


Figure 5 Comparison of displacement thickness when the jet is on and off

Effectiveness of SJA

Effectiveness of a SJA can be evaluated in various ways. To evaluate the effectiveness of a SJA on resisting flow separation, the boundary layer displacement thickness can be used. According to the identification methods developed by Hatman and Wang [6], the displacement thickness in laminar separation has a maximum value which occurs at the onset of the transition, and the maximum turbulence level occurs at the first reattachment point. The boundary layer condition in the current study belongs to the laminar separation-short bubble. Figure 5 shows the comparison of displacement thicknesses in the conditions with the synthetic jet on and off. As shown in Figure 5, the maximum displacement is at about $x = 115$ mm downstream of the SJA when the jet is off. According to the identification method in [6], this position with the maximum displacement thickness should be the onset of the transition in laminar separation. However, this maximum displacement point is hardly noticeable when the SJA is on, as the transition mode has been changed from non-frictional separation laminar separation to frictional transition. It is more difficult to define the maximum

turbulence level than to define the maximum displacement at a particular x position. However, the fluctuating velocity at $x = 140$ mm in Figure 4 may be recognized to be greater than that at other x positions. Therefore, the reattachment point should be at a position between $x = 120$ mm and $x = 140$ mm.

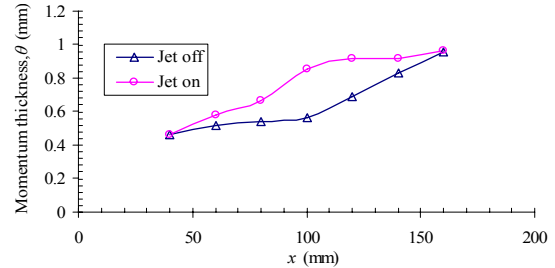


Figure 6 Comparison of momentum thickness when the SJA is on and off

The other boundary layer property, momentum thickness, may also be useful for understanding the physics associated with the effectiveness of a SJA on resisting flow separation. As we know, flow separation occurs over the surface of a wall because of momentum loss in the boundary layer with adverse pressure gradient. Comparison of the momentum thicknesses in Figure 6 shows that the SJA increases the momentum transfer from the external potential flow to the boundary layer, so that the boundary layer flow becomes more capable to support the adverse pressure gradient and not to be unattached from the wall.

The strategy of using SJAs in controlling boundary layer flow separation is to disturb the boundary layer flow and accelerate the transition from laminar to turbulence which has greater momentum than laminar flow to resist flow separation. Therefore, the level of disturbance originated by a SJA may be used to evaluate the effectiveness of the SJA. Intensity of disturbance, originally defined for measuring the ‘degree of disturbance’ in the external flow [14], is quoted here for quantitatively evaluate the effectiveness of a SJA on the level of disturbance it generates.

$$I_d = \int_0^\delta u' dy \tag{2}$$

Where I_d is the intensity of disturbance, u' is the fluctuating velocity defined in Eq. (1), y is normal-to-wall direction and δ is the local boundary layer thickness. Figure 7 compares the intensity of disturbance along the streamwise centerline in the separation zone when the SJA is switched off and on. In the case of jet off, the disturbance intensity is very small, $0.23 \text{ m}^2/\text{s}$ to $0.40 \text{ m}^2/\text{s}$, in the laminar separation region upstream of the transition point. It then suddenly starts to increase rapidly around $x = 100$ mm and does not reach the maximum value at the last measurement station. In the case of jet on, the disturbance intensity is already as large as $1.27 \text{ m}^2/\text{s}$ at the first measurement station of $x = 40$ mm. It increases linearly until it becomes steady at $x = 100$ mm. This comparison shows that the SJA works very effectively to generate the disturbance which strategically prevents the flow from separation.

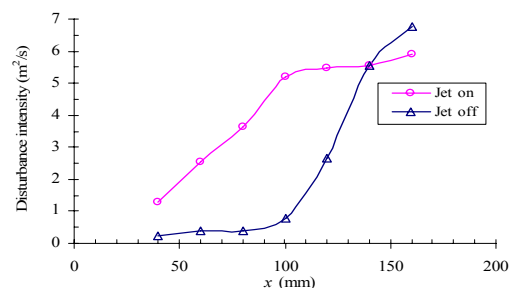


Figure 7 Comparison of intensity of disturbance when SJA is on and off

T-S and K-H Instability

K-H instability is known as a non-viscous instability associated with the laminar separation in a boundary layer under adverse pressure gradient, while T-S instability is known as a viscous flow instability playing a significant role in the transition at a zero pressure gradient. As shown in Figure 4 and identified in Figure 5, the effective actuation of the synthetic jet was realized when the actuator was driven at a T-S frequency. It was believed that the T-S waves, triggered by the synthetic jet and enhanced by the natural instability of the base flow, effectively stopped the flow separation [9]. In the model development for boundary layer separation, Hatman and Wang assumed that the transition to turbulence in separated boundary layer be a result of the superposition of the effects of K-H instability and T-S instability [6]. The fluctuating velocity profiles in the separation zone in Figure 4(b) and the I_d in Figure 7 verify this assumption.

As found in our earlier studies [10], when a synthetic jet was injected in a quiescent condition (without a cross flow), the jet velocity and momentum were maximum at a forcing frequency equal to the resonant frequency of the membrane material of the actuator. However, when the synthetic jet is injected into a boundary layer flow (with a cross flow), whether the disturbance triggered by this small jet is going to be amplified or damped depends on the interaction between the jet and the baseline flow.

Figure 8 shows the variation of the mean velocity with the forcing frequency in the condition with and without crossflow. In the case without crossflow, the velocity was measured at a position $y/d = 1.5$ along the centerline of the orifice of the SJA. Here d is the diameter of the orifice. $y/d = 1.5$ was chosen because the maximum mean velocity appeared at this position [10]. The forcing voltage without crossflow was $\pm 7.5V$. The peak mean velocity occurs at a frequency of 1.5 kHz. In the low frequency bandwidth, a secondary peak velocity with much smaller amplitude of the mean velocity appears in the range of 100–300 Hz. In the case with cross flow, as shown in Figure 8(b), the velocity was measured at $y = 0.8$ mm or $y/\delta = 0.05$ and $x = 100$ mm downstream of the SJA. This position was chosen because it was where the maximum fluctuating velocity was detected, and at the x position just upstream of $x = 115$ mm where the maximum displacement occurred, as identified with Figure 5.

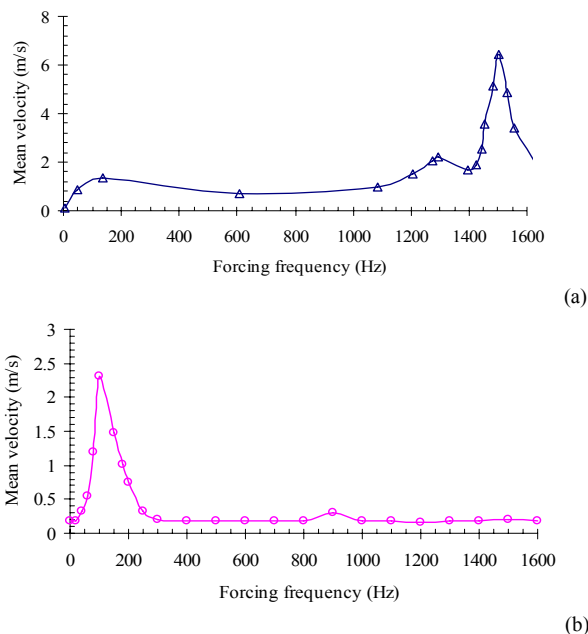


Figure 8 Mean velocity varied with the forcing frequency
a) without cross flow at $y/d = 1.5$,
b) with cross flow at $y/d = 0.8$ and $x = 100$ mm.

Therefore $x = 100$ mm was the last measurement station to show the effectiveness of the T-S waves triggered by the synthetic jet before the turbulent transition. Compared with that in Figure 8(a), the mean velocity in the lower frequency range, 60–200 Hz, in Figure 8(b) is significantly greater. The peak mean velocity in Figure 8(b) occurs at the forcing frequency of 100 Hz. The secondary peak of the mean velocity, whose amplitude is very small, occurs at 900 Hz which is the lowest resonant frequency of the membrane material of the SJA. This shows that, with crossflow, the synthetic jet at lower forcing frequencies is much more effective than that at higher forcing frequencies in the condition of the present study.

Why were the T-S waves enhanced rather than damped in our experiments? How did the T-S waves triggered by the synthetic jet interact with the K-H instability of the base flow? The following discussion may lead to or provide some answers.

The potential of closed laminar separation region to act as a generator of disturbance was identified by Gaster [2] and this identification has been recognized as a significant theoretical development [15]. In a special application of using flapping to control water separation flow in a boundary layer, Rist hypothesized three new mechanisms. One of his hypothesized mechanisms was that a laminar separation bubble itself might act as a resonator with respect to low frequency, long wave

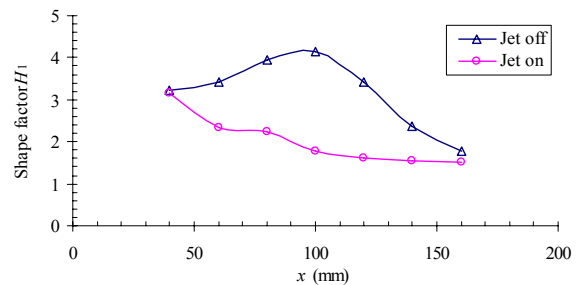


Figure 9 Comparison of shape factors when the jet is on and off

length disturbances which should be of the size of the bubble length [13]. Our experimental results positively support this hypothesis. Based on the results in Figures 4 and 5, the length of the separation bubble is identified to be in a range between 60 mm (lower limit) and 100 mm (upper limit). Calculated with the local external velocity, the hypothesized resonating frequency should be in the range of 82 Hz to 141 Hz. The forcing frequency for the results of effective synthetic jets shown in Figure 4 is 100 Hz which is within the range of resonating frequency calculated based on Rist's hypothesis. It is in fact numerically and physically equivalent to the most effective forcing frequency calculated with the reduced frequency of 1.0 if the bubble length is taken as the characteristic length. Therefore, the idea is to use the separation bubble and the associated K-H instability as an amplifier of disturbance whose frequency may be determined by the physics of the separation bubble in the baseline flow.

Figure 9 compares the shape factors in the separation bubble region when the synthetic jet was switched on and off, corresponding to the results in Figure 4. In the baseline flow when the synthetic jet is switched off, the shape factor is increasing and the separation flow is formed until the position of transition. When the synthetic jet is switched on, the shape factor is decreasing and the separation is avoided. Shape factor is interpreted physically as the ratio of the pressure forces to viscous forces. As shown in Figure 9, when this ratio is sufficiently big (>3) in the case of jet off, the pressure force is significantly greater than the viscous force, so that the viscous

force is unable to keep the flow attached to the wall and the K-H instability plays a dominating role in the boundary layer until the transition to turbulence. In this sense, K-H and T-S instabilities compete to each other if both of these two instabilities exist in the boundary layer. However, the K-H instability can also play a role to enhance the T-S instability triggered by synthetic jets. As shown in Figure 9, in the case of jet on, the adverse pressure gradient and the associated K-H instability provide strong amplification to the T-S waves triggered by the SJA prior to the breakdown to nonlinearity. The amplified T-S waves replace the dominating role and reduce the ratio of the pressure force to viscous force to be less than three (<3), so that the pressure force is not sufficient to separate the flow from the wall. This may suggest that the effective forcing frequency of a SJA should be determined with consideration of mainly the instability (both T-S and K-H) of the base flow and also of the vibrating properties of membrane material of the SJA.

Conclusions

A SJA with an exit orifice of 500 μm was applied to laminar separation caused by adverse pressure gradient in a boundary layer. Sample experimental results at a low forcing voltage of $\pm 7.5\text{V}$ and low forcing frequency of 100 Hz demonstrated successful elimination of a laminar separation bubble. Boundary layer properties were used to identify this elimination of laminar separation, and the intensity of disturbance which was the integration of velocity fluctuation over the boundary layer was used to show the SJA's effectiveness on generating the turbulence which resisted the flow separation.

Analysis of the experimental results leads to the conclusion that the flow instability plays an important role in enhancing the effectiveness of the SJAs and also making the control effectiveness less dependent of the actuator. To enable a micro synthetic jet actuator to work effectively on preventing the boundary layer flow from laminar separation, the key issue is to use the synthetic jet actuator as an instability trigger to trigger T-S instability which resonates with the K-H instability of the baseline flow to accelerate the viscous transition. The triggered T-S waves are amplified and enhanced by the non-viscous K-H instability of the baseline flow and consequently become effective in controlling the K-H instability. As a trigger rather than a force generator, the synthetic jet actuator should actuate independently to its size and weight.

Acknowledgments

The author wishes to acknowledge the assistance provided by C. Lee to the experimental work. The advice provided by Prof. J. P. Gostelow on T-S instability in 2001 and by Prof. I. Wygnanski on K-H instability in 2002 is gratefully appreciated.

References

- [1] Amitay, M., Smith, D., Kibens, V., Parekh, A. and Glezer, A., "Aerodynamic flow control over an unconventional airfoil using synthetic jet actuators" AIAA Journal, Vol. 39, No. 3, pp. 361-370, March 2001.
- [2] Gaster, M., "The Structure and Behaviour of Laminar Separation Bubbles", A.R.C. R&M Report No. 3595, 1969.
- [3] Gilarranz, J.L., Traub, L.W. and Rediniotis, O.K., "A New Class of Synthetic Jet Actuator – Part I: Design, Fabrication and Bench Top Characterization", ASME J. Fluids Eng., 127, pp. 367-376, March 2005.
- [4] Gilarranz, J.L., Traub, L.W. and Rediniotis, O.K., "A New Class of Synthetic Jet Actuator – Part II: Application to Flow Separation Control", ASME J. Fluids Eng., 127, pp. 377-387, March 2005.
- [5] Glezer, A. and Amitay, M., "Synthetic jets", Annu. Rev. Fluid Mech., 34:503-29, 2002.
- [6] Hatman, A. and Wang, T., A prediction model for separated-flow transition, ASME Paper, GT-98-237, ASME Turbo Expo '98, Stockholm, Sweden, 1998.
- [7] Ho, C.M. and Tai, Y.C., "Review: MEMS and its applications for flow control", ASME Journal of Fluids Engineering, Vol. 118, pp.437-447, September 1996
- [8] Hong, G. "Effectiveness of micro synthetic jet actuator enhanced by flow instability on controlling laminar separation caused by adverse pressure gradient", Sensors and Actuators A: Physical, Vol.132, Issue 2, pp.607-615, 2006.
- [9] Hong, G., Lee, C., Ha, Q., Mack, A.N.F., Mallinson, S.G., "Effectiveness of synthetic jets enhanced by instability of Tollmien-Schlichting waves", AIAA paper 2002-2832, 1st AIAA Flow Control Conference, St Louis, Missouri, USA, 24-26 June 2002.
- [10] Hong, G., Mallinson, S.G., Lee, C. and Ha, Q.P., On Centerline Distributions Of the Mean Velocity in Synthetic Jets, Proceedings of 14th Australasian Fluid Mechanical Conference, Adelaide, Australia, December 2001.
- [11] Huang, A., Ho, C.M., Jiang, F., Tai Y.C., "MEMS transducers for aerodynamics—a paradigm shift," AIAA 00-0249, 2000.
- [12] Pilon, A., "Aerospace Science", Aerospace America, pp13-16, December 2004.
- [13] Rist, U., "Instability and transition mechanisms in laminar separation bubbles", VKI/RTO-LS Low Reynolds Number Aerodynamics on Aircraft including Applications in Emerging UAV Technology, Rhode-Saint-Gense, Belgium, 24-28 November 2003.
- [14] Schlichting, H. (Translated by Kestin, J.), Boundary-Layer Theory, 7th Edition, McGraw-Hill, 1979.
- [15] Seifert, A. Theofilis, V., Joslin, R.D., "Issues in active flow control: theory, simulation and experiment", AIAA 2002-3277, 1st AIAA Flow Control Conference, St Louis, Missouri, USA, 24-26 June 2002.